Inorganic Chemistry

ARTICLE

pubs.acs.org/IC

Relativistic Effects and Gold Site Distributions: Synthesis, Structure, and Bonding in a Polar Intermetallic $Na_6Cd_{16}Au_7$

Saroj L. Samal and John D. Corbett*

Ames Laboratory-DOE and Department of Chemistry, Iowa State University, Ames, Iowa 50010, United States

Supporting Information

ABSTRACT: $Na_6Cd_{16}Au_7$ has been synthesized via typical high-temperature reactions, and its structure refined by single crystal X-ray diffraction as cubic, $Fm\bar{3}m$, $a = 13.589(1)$ Å, $Z = 4$. The structure consists of Cd_8 tetrahedral star (*TS*) building blocks that are face capped by six shared gold (Au2) vertexes and further diagonally bridged via Au1 to generate an orthogonal, three-dimensional framework $[Cd_8(Au2)_{6/2}(Au1)_{4/8}]$, an ordered ternary derivative of Mn_6Th_{23}. Linear muffin-tin-orbital (LMTO)-atomic sphere approximation (ASA) electronic structure calculations indicate that $Na_6Cd_{16}Au_7$ is metallic and that ~76% of the total crystal orbital Hamilton populations (−ICOHP) originate from polar Cd−Au bonding with 18% more from fewer Cd−Cd contacts. $Na_6Cd_{16}Au_7$ (45 valence electron count (*vec*)) is isotypic with the older electron-richer $Mg_6Cu_{16}Si_7$ (56 *vec*) in which the atom types are switched and bonding characteristics among the network elements are altered considerably (Si for Au, Cu for Cd, Mg for Na). The earlier and more electronegative element Au now occupies the Si site, in accord with the larger relativistic bonding contributions from polar Cd−Au versus Cu−Si bonds with the neighboring Cd in the former Cu positions. Substantial electronic differences in partial densities-of-states (PDOS) and COHP data for all atoms emphasize these. Strong contributions of nearby Au $5d^{10}$ to bonding states without altering the formal *vec* are the likely origin of these effects.

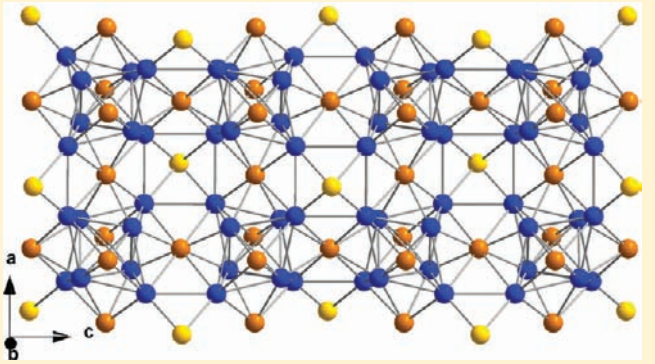

INTRODUCTION

New polar intermetallic compounds give us an increasingly rich variety of novel structures with diverse cluster and network chemistry and unusual bonding patterns. These compounds occur between two or more metallic elements, often with widely different Mulliken electronegativities. The intermetallic compounds may be classified into two subgroups: polyatomic cationic networks with simple monoanions and polyanionic networks with simple cations.[1] Classical examples of the latter are polyatomic networks of reduced p elements, mainly those from groups 14−16, combined with alkali or other active metals in Zintl (valence) phases. A wide variety of newer intermetallic chemistry arises when electron poorer group 13 *triels* (Tr), group 12 (*diels*), or even earlier elements such as late transition metals (or both) are introduced. The heavier triels In and Tl in relatively alkali-metal-rich binary systems initially led to either Tr clusters or networks.[2,3]

Among the sixth period transition elements, gold in formal negative oxidation states forms a fascinatingly wide variety of compounds with remarkable structural diversities. The redox nobility of the unique element gold is related to the marked contraction of its atomic size as a result of the relativistic effects.[4] Numerous new compounds with unusual structures and short and apparently strong Au−Tr bonds have been discovered during explorations in the (*A*/*Ae*)−Au−Tr systems (*A* = alkali metal, *Ae* = alkaline-earth-metal).[5−12] On the other hand, less success has been obtained with earlier and electron-poorer elements such as Cd, Zn, Cu, and so forth in place of Tr.[13−15] For example, attempts to substitute some Cu or Zn group elements in place of Ga in $RbGa_3$ were unsuccessful, although gold did substitute for 12% of the Ga.[14] The substitution of electron-poorer (Cu or Zn group) elements into binary (*A*/*Ae*)−Tr systems has been less productive, leading to more condensation into clusters.[13,14]

Several rare-earth-metal(R)-based ternary cadmium compounds (*R*−*Tn*−Cd; *Tn* = transition metal) have been reported recently.[16−19] Pd@R_6 octahedra are the basic motifs in palladium-rich $R_6Pd_{13}Cd_4$[17] compounds whereas *Tn*-centered trigonal prisms of *R* atoms and Cd_4 tetrahedra are basic building blocks in *R*-rich ternary cadmium compounds $R_{23}Tn_7Cd_4$ and R_4TnCd.[18,19] Less is known about *A*/*Ae*−Au−Cd systems, the only example being with Ca.[15,20] For CaAu, 11% of the Au is substituted by Cd in a disordered orthorhombic CrB structure, and a cubic CsCl structure type forms above 70% Cd.[20] There are three more phases in the Ca−Au−Cd system. In $CaCd_xAu_{2-x}$, $x = 0.76-1.00$, the compound crystallizes in an ordered variant of the KHg_2 structure type. A line compound $Ca_5Cd_2Au_{10}$ with a

Received: March 10, 2011
Published: July 05, 2011

Table 1. Selected Crystal Data and Structure Refinement Parameters for $Na_6Cd_{16}Au_7$

compound	$Na_6Cd_{16}Au_7$
formula weight	3315.26
space group, Z	$Fm\bar{3}m$, 4
unit cell parameter (Å)	13.589(1)
V (Å^3)	2509.4(5)
d_{calcd} (g cm^{-3})	8.775
crystal size (mm^3)	0.05 × 0.03 × 0.04
θ range for data collection	2.60 to 28.27°
index range	$-18 \le h \le 17$, $-17 \le k \le 17$, $-18 \le l \le 18$
reflections collected	5563
indep. obs. reflections (R_{int} = 0.0455)	200
μ/mm^{-1}(Mo Kα)	54.05
data/params	200/15
$R1/R_w$ ($I > 2\sigma$ (I))	0.0187/0.0418
(all data)	0.0187/0.0418
largest diff. peak, hole,e Å^{-3}	+ 3.51 [2.83 Å from Na] and −0.88 [1.06 Å from Au2]

Zr_7Ni_{10} structure type is known in the gold-richer region, and $Ca_{11}Cd_{18+x}Au_{4-x}$ (studied for $x = 0$ and 0.6) has a new structure type, tetragonal $I4_1/amd$ in the Cd-richer part.[15] The basic framework in the former $Ca_5Cd_2Au_{10}$ consists of sinusoidal Au layers stacked along the b-axis, as in $Ca_4In_3Au_{10}$ structure,[21] with the Ca and Cd atoms sandwiched between the layers, whereas the structure of $Ca_{11}Cd_{18}Au_4$ contains wavy layers of pentagonal antiprisms built of cadmium and gold atoms.[15] Several compounds are also known in the Sr−Au−Cd system.[15,20]

Expanding our exploratory syntheses into the Na−Au−Cd system allowed the discovery of the new $Na_6Cd_{16}Au_7$, the first ternary compound in this system. The nominally isostructural but electron richer (and somewhat nonstoichiometric) $Mg_6Cu_{16}Si_7$ is also known,[22,23] these being the only ordered ternary variants of the Th_6Mn_{23} structure type known. Variants ($Ca_6Li_{11}Al_{12}$,[24] $Pr_6Ag_{13}Al_{10}$,[25] La_6AlMg_{22}[26]) that are disordered in the *Mn*- sites occupancies have also been reported.

EXPERIMENTAL SECTION

Synthesis. Gold (99.995%, Ames Lab) and cadmium (99.99%, Alfa Aesar) were used as received whereas the surface of the sodium metal (99.9%, Alfa) was cleaned with a scalpel before use. Stoichiometric amounts of the elements were weld-sealed within a tantalum container and subsequently enclosed in an evacuated silica jacket to protect the Ta from air. These were allowed to react at 600 °C for 15 h before quenching, then equilibrated at 400 °C for 4 d, and cooled to room temperature. The synthesis conditions were similar to general methods employed earlier.[5−9,27]All the reactants and products were handled in a glovebox filled with dry N_2 (≤0.1 ppm H_2O per volume). Crystals of the compound was first encountered during a reaction of the composition $NaCd_2Au$, and were synthesized X-ray pure (Supporting Information, Figure S1) once the correct composition was realized. The compound has a metallic luster and readily decomposes in moist air at room temperature to hydroxides and gold. To check for any homogeneity range around the composition $Na_6Cd_{16}Au_7$, samples with excess Cd ($Na_6Cd_{17}Au_7$) and excess Au ($Na_6Cd_{16}Au_8$) were synthesized by the same procedure, after which the cubic lattice parameters were found to vary only very minor amounts, 0.011(2) Å overall (1:10^4; Guinier data; Supporting Information, Table S1), and no diffraction lines for foreign phases could be found. A significant phase field region was found for $Na_6Cd_{16}Au_7$, Supporting Information, Figure S2. It is notable that attempts to synthesize the K and Rb analogues were unsuccessful. Also, compositions with higher gold content do not form any discernible ternary variant of Th_6Mn_{23} or of any other phase type.

X-ray Diffraction Studies. Powder diffraction data were collected at room temperature with the aid of a Huber 670 Guinier powder camera equipped with an area detector and Cu K_α radiation (λ = 1.54059 Å). The samples were dispersed between two Mylar sheets with the aid of a little vacuum grease and in turn held between split Al rings that provided airtight seals. The lattice parameters were refined using the WinXPow program.[28]

Single crystals of $Na_6Cd_{16}Au_7$ grown by annealing at 400 °C in Ta were subsequently sealed in capillaries within a N_2-filled glovebox. Single-crystal diffraction data sets were collected from one at room temperature from three sets of 606 frames with 0.3° scans in ω and exposure times of 10 s per frame with the aid of a Bruker SMART CCD diffractometer equipped with Mo K_α radiation (λ = 0.71073 Å). Systematic extinctions indicated an *F*-centered cubic lattice. The reflection intensities were integrated with the SAINT program in the SMART software package[29] over the entire reciprocal sphere to 2θ = 56.5°. The unit cell dimension a = 13.589(1) Å was obtained from least-squares refinement of 33 lines in the Guinier powder pattern. Empirical absorption corrections were made with the aid of the SADABS program.[30] The space group determination was done with the aid of XPREP and SHELXTL 6.1.[31] The structure was solved by direct methods and subsequently refined on $|F^2|$ with a combination of least-squares refinement and difference Fourier maps with the aid of the SHELXTL 6.1 software package in the indicated centro-symmetric space group $Fm\bar{3}m$ (R_{int} = 0.049), ultimately with anisotropic displacement parameters. Some details of data collection and refinement parameters are given in Table 1, the atom positional data are given in Table 2, and the anisotropic displacement parameters are in the Supporting Information, Table S2. Important bond distances are in listed in Table 3 and Supporting Information, Table S3, and the observed powder pattern is compared with that calculated on the basis of the refined structure in Supporting Information, Figure S1. The cif output and a summary of parameters are also provided in the Supporting Information.

Electronic Structure Calculations. Tight binding calculations for $Na_6Cd_{16}Au_7$ were performed according to the linear muffin-tin-orbital (LMTO) method in the atomic sphere approximation (ASA).[32] The radii of the Wigner−Seitz spheres were assigned automatically so that the overlapping potentials would be the best possible approximations to the full potentials.[33] No additional empty spheres were needed subject to a 16% overlap restriction for atom-centered spheres. Basis sets of Na 3s,3p,(3d), Au 6s,6p,5d,(5f), Cd 5s,5p,4d,(4f) (downfolded

dx.doi.org/10.1021/ic200501h |*Inorg. Chem.* 2011, 50, 7033–7039

orbitals in parentheses) were employed, and the reciprocal space integrations were carried out using the tetrahedron method. Scalar relativistic corrections were included. Calculations were also performed on $Na_6Au_7Cd_{16}$ with Cd $4d^{10}$ as core inasmuch as artificial Cd 4d−Au 5d coupling appeared to be significant otherwise (below). For bonding analysis, the energy contributions of all filled electronic states for selected atom pairs were calculated by the COHP method (crystal orbital Hamilton population),[34] and the energy-weighted −ICOHP sums up to E_F per bond type were also calculated to give Hamilton populations (Supporting Information, Tables S3 and S4).

RESULTS AND DISCUSSION

Structure. The most remarkable features of $Na_6Cd_{16}Au_7$ are the high coordination numbers and large bond populations among these particular elements. Its structure (space group: $Fm\bar{3}m$; a = 13.589(1) Å) is illustrated in Figure 1, and the distances and Hamilton populations (−ICOHP) are summarized in Table 3 and Supporting Information, Table S3. (All atom environments are shown in the Supporting Information, Figure S3.) The basic building blocks in this compound are cadmium tetrahedral stars (*TS*) (Cd_8, blue), which are often encountered in intermetallics, more specifically among electron-poorer compounds (valence electron counts (*vec*) = 2.1−2.6 e/atom).[35,36] A *TS* may be simply described in term of an inner tetrahedron that is further face capped by a larger inverted tetrahedron, often of the same element. In $Na_6Cd_{16}Au_7$, Cd2 and Cd1 define the inner and outer tetrahedra, respectively. The *TS* units lie at the octant centers ($\pm^1/_4$, $^1/_4$, $^1/_4$) and have 222 (D_{2d}) symmetry. The tetrahedra, d(Cd−Cd) = 3.078 and 3.303 Å are moderately distorted from the ideal, reflecting differences in the number of bonded Cd neighbors to each (Figure 1c).

Additional heteroatomic Cd−Au bonding evidently makes this array particularly stable. The *TS* are interbonded via six Au2 (*m.mm*) atoms (orange), each of which bonds between quadrilateral faces of a pair of *TS* parallel to the cell axes, Figure 2a. Parallel *TS* are also interbonded at Cd1 (d(Cd1−Cd1) = 3.227 Å) along axial directions, and finally, the empty Cd_8 polyhedra are bridged by Au1 ($m\bar{3}m$) (yellow) atoms that lie on the centers of the cell edges and also bond exo to eight Cd1 atoms of eight *TS*, Figure 2b. The gold and cadmium atoms define an infinite $[Cd_8(Au2)_{6/2}(Au1)_{4/8}]_2$ network in which sodium atoms form zigzag and linear chains with alternate electronegative gold atoms.

The structure may also be approximated geometrically in terms of fused 26-atom clusters,[37] without giving much attention to chemical bonding differences. This has the advantage of describing a complicated structure on the basis of a set of polyhedra. The 26-atom clusters are centered at the octant positions, Figure 3a, each built of three different polyhedra, a *TS* unit of Cd_8, which is both encapsulated by an octahedron (OH) of six Au2 atoms (along axial directions), and surrounded by a cube-octahedron (CO) of 12 Na atoms. Finally, these clusters are shared along the cell axes via the six planar rectangular faces of the CO, each of which consists of four sodium atoms centered by

Table 2. Atomic Coordinates and Isotropic Equivalent Displacement Parameters for $Na_6Cd_{16}Au_7$

atom	Wyckoff	symmetry	x	y	z	U_{eq}
Au1	4*b*	$m\bar{3}m$	0.5	0.0	0.0	0.0122(3)
Au2	24*d*	*m.mm*	0.25	0.25	0.00	0.0165(2)
Cd1	32*f*	3*m*	0.3813(1)	0.1187(1)	0.1187(1)	0.0160(3)
Cd2	32*f*	3*m*	0.3359(1)	0.3359(1)	0.1641(1)	0.0173(3)
Na	24*e*	4*m.m*	0.2080(7)	0.0	0.0	0.025(1)

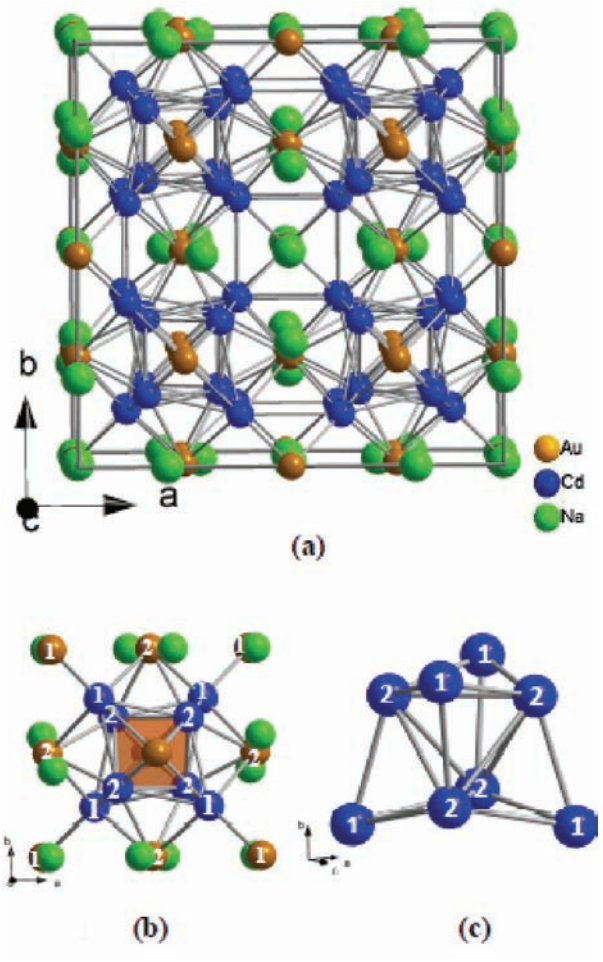

Figure 1. (a) Structure of $Na_6Cd_{16}Au_7$ constructed from Cd_8 (blue), each of which consists of inner Cd2 tetrahedra face-capped by larger Cd1 tetrahedra. These *TS* are further face-capped by six Au2 atoms (orange). (b) The basic *TS* building blocks in $Na_6Cd_{16}Au_7$ along with all nearest neighbors. (c) The moderately distorted TS; d(Cd2−Cd2) = 3.303 Å, d(Cd1−Cd2) = 3.078 Å.

Table 3. Bond Length Ranges and Average −ICOHP Values in $Na_6Cd_{16}Au_7$

bond type	lengths (Å)	−ICOHP (eV/per bond. mol)	*n*/cell	−ICOHP (eV/cell)	contribution (%)
Au−Cd	2.775−2.995	1.296	16	20.74	76.1
Cd−Cd	3.078−3.303	0.534	9	4.81	17.6
Na−Cd	3.209−3.279	0.160	8	1.28	4.7
Na−Au	3.445	0.111	4	0.45	1.6

dx.doi.org/10.1021/ic200501h |*Inorg. Chem.* 2011, 50, 7033–7039

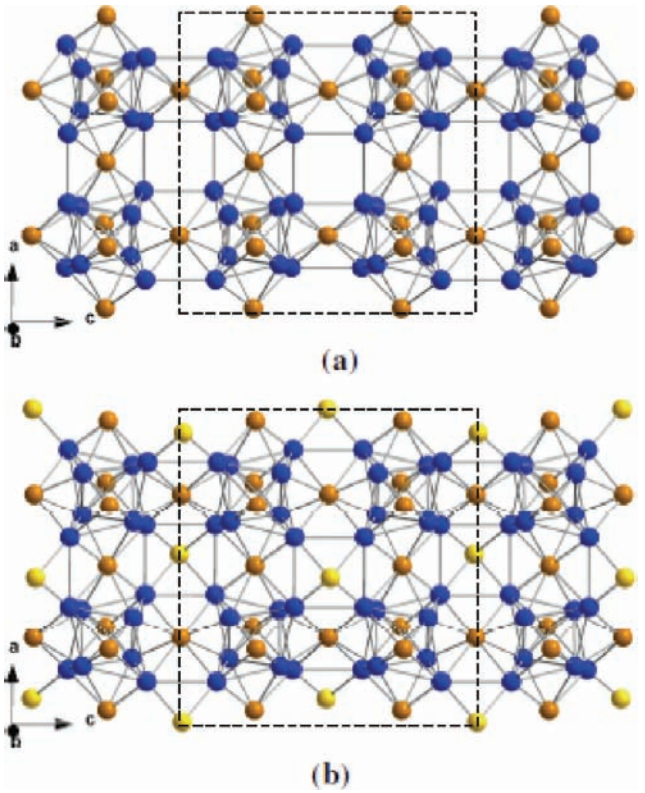

Figure 2. Anionic Au−Cd framework $[Cd_8(Au2)_{6/2}(Au1)_{4/8}]$ of $Na_6Cd_{16}Au_7$. (a) TS of Cd_8 (blue) face capped by six Au2 atoms (orange) (Au1 and Na atoms are omitted). (b) The face capped *TS* units are further corner bridged at Cd1 atoms by Au1 (yellow) atoms (Na atoms are omitted).

the Au2 atom, Figure 3b. The Au1 atoms are present in octahedral holes at $(^1/_2,0,0)$ (Wyckoff 4*b*), the interstices between the multiclusters, with eight Cd1 neighbors from the outer tetrahedra of the eight surrounding clusters.

All interatomic distances in $Na_6Cd_{16}Au_7$ appear in the Supporting Information, Table S3. The sodium atoms are surrounded by 12 neighbors, four Cd1, four Cd2, and four Au2 atoms (Supporting Information, Figure S3). The Na environment is better described as an off-centered square prism of eight Cd atoms that is also waist-capped by four Au2 atoms. The Na−Cd distances vary only slightly, 3.209 Å to 3.279 Å. The two gold atoms both lie in special positions. The Au1 in a 4*b* position has a cubic environment with eight Cd1 neighbors whereas each Au2 in a 24*d* position has 12 neighbors: four Cd1, four Cd2, and four Na atoms at the vertices of a distorted (regular) icosahedron. The Cd−Au distances range over 2.775 Å−2.995 Å, paralleling the coordination numbers, and are comparable to the 2.829 Å−2.916 Å separations in CaAuCd in which Au has nine neighboring atoms.[15] The Cd2 atoms are also icosahedrally surrounded by three Na, three Au2, three Cd1, and three Cd2 atoms, whereas Cd1 has 13 neighboring atoms, three Na, four Au, three Cd1, and three Cd2. Both cadmium positions have only mirror symmetry. Recall also that this compound must be quite close to a line compound inasmuch as no dimensional evidence for any significant mixed or partial site occupancy could be induced by compositional variations in the syntheses, in contrast to some of its neighbors (Supporting Information, Table S1).[22,24]

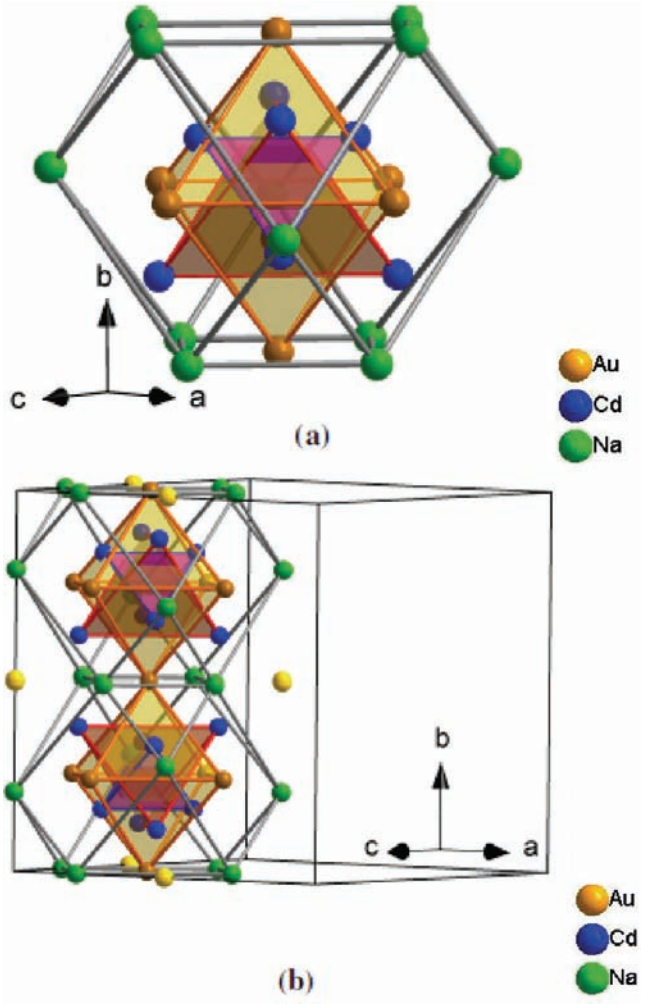

Figure 3. Approximant description of the structure of $Na_6Cd_{16}Au_7$ from (a) alternate fused 26-atom clusters (Au1 atoms omitted); (b) 26-atom clusters centered at the octant positions of the cubic cell that share faces of square planar sodium atoms (green) and extend along all three axial directions. The Au1 atoms (yellow) occupy the interstices between the clusters.

The structures of $Na_6Cd_{16}Au_7$ and its binary counterpart Th_6Mn_{23} are very similar to that of $Sc_{11}Ir_4$[37] and occur in the same space group, $Fm\bar{3}m$. $Sc_{11}Ir_4$ may be written as $Sc_6Sc_{16}Ir_7Ir$, a stuffed variant of $Mg_6Cu_{16}Si_7$-type in which an additional 4*a* site is also filled by Ir. Two other filled variants of Th_6Mn_{23}-type have also been reported, $Ti_6Al_{16}AlFe_7$ and $Ti_6Ni_{16}Si_7Si$ in which the same 4*a* site is occupied.[38] In $Ti_6Ni_{16}Si_7Si$, the more electronegative Si atoms occupy the 4*a*, 4b, 24d sites, whereas, in $Ti_6Al_{16}AlFe_7$, Al atoms occupy two 32*f* sites and 4*b* site, displacing the (more electronegative) Fe to the 4*a* site. Note that no ternary variant of $Sc_{11}Ir_4$ was found in Na−Au−Cd system.

Electronic Structure and Bonding. The total densities-of-states (DOS), individual atom projections, and the orbital projections for each atom type in $Na_6Cd_{16}Au_7$ (per cell) are shown in Figures 4A(a−d) along with the subsequent −COHP data (part e) for each bond type., These result from the more meaningful output of a second calculation, Figure 4A, in which the Cd $4d^{10}$ orbitals were treated as core, in view of the unusual coupling artifacts between nominal Cd 4d (∼ −9.5 eV), sodium,

dx.doi.org/10.1021/ic200501h |*Inorg. Chem.* 2011, 50, 7033–7039

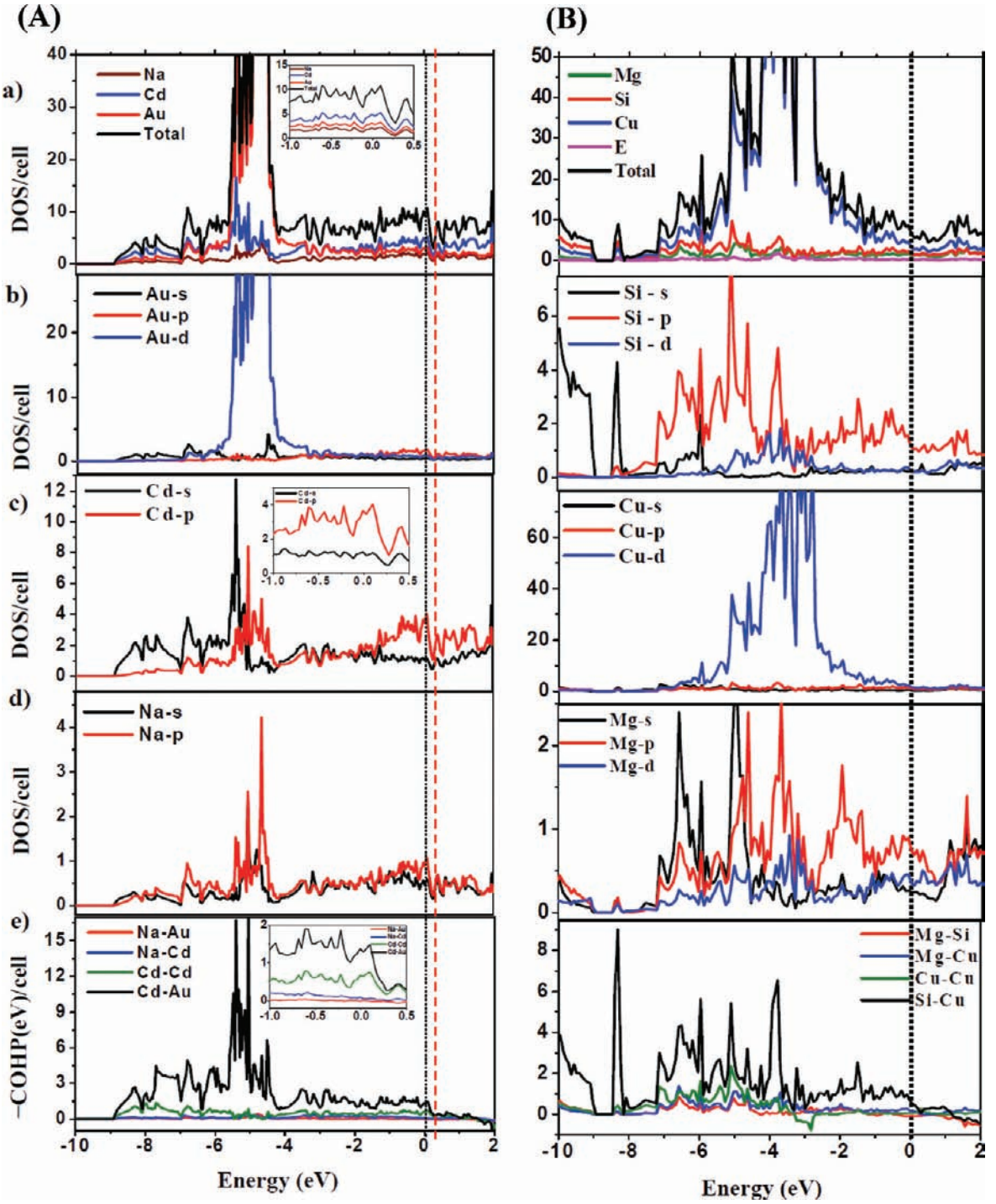

Figure 4. Results of LMTO-ASA calculations for (**A**) $Na_6Cd_{16}Au_7$ cell (E_F in black) considering Cd-4d as core and (**B**) $Mg_6Cu_{16}Si_7$(E_F in black). (a) Densities of states (DOS) for different atom types. (b) Partial projections of orbital components Au 5d, 6s, 6p or Si 3d, 3s, 3p. (c) Same for Cd 5s, 5p or Cu 3d, 4s, 4p. (d) Same for Na 3s, 3p or Mg 3s, 3p, 3d. (e) −COHP values (eV per cell) for Au−Cd (black), Cd−Cd (green), Na−Cd (blue), and Na−Au (red) interactions or Si−Cu, Cu−Cu, Mg−Cu, and Mg−Si interactions. Note the scale expansions in insets.

and gold 5d that appeared throughout the first set of results, Supporting Information, Figure S4.

All of the data support a rather regular assessment of the bonding in this compound, most directly in terms of the −COHP (Figure 4Ae) and −ICOHP (Table 3) data, but in the DOS as well as far as the dominance of the Au−Cd (and Cd−Cd) bonding throughout, even up to E_F (see black curves in Figure 4Aa,e. The Na contributions are barely evident at the COHP level, rather only in PDOS. A closer look at the states around E_F suggest that the phase may at best be a poor metal and that the orbital contributions are somewhat ordered radially.

The (Au,Cd) DOS values decrease quite noticeably at E_F for the refined composition (115 valence e^- per formula unit), and this is immediately followed by what might at first be viewed a

dx.doi.org/10.1021/ic200501h |*Inorg. Chem.* 2011, 50, 7033–7039

Table 4. Bond Length Ranges and Average −ICOHP Values in $Mg_6Cu_{16}Si_7$[22]

bond type	length (Å)	−ICOHP (eV/per bond mol)	*n*/cell	−ICOHP (eV/cell)	contribution (%)
Si−Cu	2.378−2.536	1.236	16	19.78	66.0
Cu−Cu	2.543−2.866	0.496	9	4.47	14.9
Mg−Cu	2.779−3.041	0.437	8	3.50	11.7
Mg−Si	3.017	0.556	4	2.23	7.4

pseudogap about 2 e^- wide (red dashed line), but this is seen to be principally defined by the p states of Cd and Na (Figure 4A). Assuming the electron count and the phase composition are valid, the filling of this valley reflects the topping up of a fairly nonbonding (and largely empty) p band, principally Na 3p and Cd 5p, at the top of the cluster binding states (Au, Cd) and do not signal any usual electronic pseudogap. (A similar situation has been deduced for the metal p-states at the top of the conduction band in the cluster chains in Pr_3RuI_3 and its neighbors).[39] This narrow interval is defined mainly by Cd−Au and Cd−Cd bonding states (−COHP), which suggest that moderate electron doping of a rather poor metal may be possible. The principal Cd 5s and 5p bonding states fall within and below the region of dominant gold 5d bonding, <∼4.0 eV). The minor Na−Au bonding role in this phase (Table 3, Figure 4) naturally correlates with the low proportions of both metals therein and the low coordination numbers to each other. This greatly contrasts with the structure-building characteristics of the cations in K_3Au_5Tr (Tr = In, Tl), and so forth in which vertex-sharing Au_4 tetrahedra also have 12 K and 2 Tr neighbors.

Some useful ideas about the overall bonding in the structure can be derived from the energy-weighted sums of the Hamiltonian populations for each bond type up to E_F (Figure 4Ae) and their relative bonding contributions over the whole cell, Table 3. Noteworthily, these reveal that ∼94% of the populations come from Cd−Au and Cd−Cd bonding, the major contributions coming from the former Cd−Au set (black, Figure 4Ae). There are three different Cd−Au distances, eight Cd1−Au1 (d = 2.795(1) Å), four Cd2−Au2 (d = 2.775(1) Å), and four Cd1−Au2 (d = 2.995 Å) per cell that are reflected in their large −ICOHP total (Supporting Information, Table S3). Cd−Au bonds provide 76.1% of the total whereas a 17.6% contribution comes from Cd−Cd. The average −ICOHP value for Cd−Cd interactions (0.53 eV/mol) is less than half that for Au−Cd (1.296 eV) and with a lower frequency, nine per cell. Although Au−Au interactions dominate in many structures,[40] this particular gold-poorer example is predominantly stabilized by the polar Cd−Au bonds, the remaining Na−Cd and Na−Au having distinctly lower populations. The accommodation of a stoichiometry to an effective high coordination packing is obviously also very important.

Some unoccupied bonding states appear above E_F in the COHP data (Figure 4Ae which suggest that moderate electron doping may be possible. To verify this we tried to introduce electron-richer elements at different sites (e.g., $Na_4Ca_2Au_7Cd_{16}$, $Na_4Mg_2Au_7Cd_{16}$, $Na_6Au_7Cd_{14}In_2$). Only the last In substitution gave a designed X-ray-pure isotype, the $0.006(2^{1/2})$ Å decrease in a being roughly the weighted difference in radii. Still higher indium substitution attempts on Cd-sites leads to other multiphasic products. It should also be noted that compositions with higher gold or cadmium content do not form any discernible ternary variant of Th_6Mn_{23} parent or of any other type. Haussermann et al.[35] have observed from tight binding calculations that several sp-bonded intermetallic phases with basic *TS* motifs have valence electron counts (*vec*) in the range of 2.1−2.6 per atom. An orbital model indicated that 2.0−2.5 valence electrons per atom are the optimal bonding states in such *TS*s,[41] and these explain the stability maxima well.[35] However, the valence electron count per atom in $Na_6Cd_{16}Au_7$. is only 1.55. This may imply that a few bonding states are unoccupied, as weakly suggested by the COHP data, but it is not clear how to incorporate these save by doping with In and so forth, although mixed site occupancies are probably destabilizing. But in practice the inclusion of gold in a phase also brings strongly bonding $5d^{10}$ states into play without the formal addition of more valence electrons, diminishing the importance of *vec* guidelines.

Although the contrasting $Mg_6Cu_{16}Si_7$ isotype (56 valence e) is the only other ordered example of this structure type, elements with the lower electronegativities generally occupy the 24*e* site in the whole family, the early active (transition) metals, Mg or *R*.[22−26] The elements with highest (Mulliken) electronegativities are usually late transition elements, Si or Al, and occupy 4*b* and 24*d* sites. In the electron-poorer $Na_6Cd_{16}Au_7$ singularity (45 valence e), this is Au. Note that the differences in extreme electronegativities are much greater in $Na_6Cd_{16}Au_7$ than in $Mg_6Cu_{16}Si_7$.[42] Hence, the primary bonding contributions to the overall structure lie in the anionic parts, whereas, contributions in $Mg_6Cu_{16}Si_7$ come from both the cation and the anion parts. This is clearly evident from the −ICOHP proportions obtained for $Mg_6Cu_{16}Si_7$, Tables 3 and 4 and Supporting Information, Figure S4: Si−Cu, 66%, Cu−Cu, 14.9%, Mg−Cu, 11.7% . However, in $Na_6Cd_{16}Au_7$ the major bonding contributions come from Cd−Au bonds (76%), and the contributions from Na−Cd and Na−Au (versus Mg−Cu and Mg−Si) are very marginal (4.7% and 1.6%, respectively).

Although such comparisons between the two compounds can never be quantitative, the relativistic roles and polar bonding seem to play important roles in the new example. On the other hand, too serious comparisons can at the same time be somewhat futile and foolish, and the comparisons, maybe rather meaningless, in particular when we seek to compare the two phases that are related only by some structural similarity. These two interesting phases are, first, considered "stable", and that statement means only one thing—" thermodynamically stable with respect to any other set of equilibrium phases in the same system". We generally have only poor ideas as to what those alternate phases might have been, especially any that may have been "second-best" compositions and structures in that particular system. The inquiry is further complicated by the fact that we are talking about two different ternary systems of, at best, modestly similar elements. Which are the most similar triads among Mg, Au, Si, Cd, Na, and Cu? Also, why have no other good examples been reported? The last is particularly hard to say, as it depends largely on investigators who chose to study the right compositions and temperature ranges and, perhaps, who either recognized the pattern type (this Mg−Cu−Si example was first assigned and

refined in 1934!) or who got a usable single crystal in later years. The present result is for us still surprising; although we did not mount a significant synthetic search, K, Rb, or Zn do give other results. Finally, close comparisons of the two isotypes we do know still leaves us quite unsatisfied as to why they both form with this structure rather than something else; the two really are quite different in relative dimensions, packing, and bonding interactions (Supporting Information). The answers and limitations probably lie with the investigators who did not persist or resort to deeper analyses.

The capabilities of gold to give strong bonding are clearly (at least) 2-fold, both originating from its exceptional relativistic effects. (1) Relatively large proportions allow particularly strong Au−Au bonding because of its reduced size and the effective participation of their 5d orbitals in these bonds. (2) Even in the minority, gold clearly exhibits strong heteropolar bonding with modestly electronegative metals or metalloids, particularly among the post transition members. The present compound reflects this well inasmuch as Au is only 24 mol % of the total. Possible intra-d-examples do not appear to have been well studied.

CONCLUSION

The first ternary compound in the Na−Au−Cd system, $Na_6Cd_{16}Au_7$, is loosely isotypic with $Mg_6Si_7Cu_{16}$ even with a 20% smaller valence electron count. Analysis of LMTO-ASA calculations reveal that the new compound is metallic in nature, and the overall bond populations are dominated by polar Cd−Au bonds. The primary bonding contributions to the overall structure come from what can be called the anion part, Cd−Au and Cd−Cd. The relativistic effects of gold, the involvement of $5d^{10}$ states, and the compact structure all play important roles in the structure stability of the electron poorer $Na_6Cd_{16}Au_7$ and the explanations.

ASSOCIATED CONTENT

Supporting Information. Tables S1 with refined lattice parameters; S2 for the displacement ellipsoid parameters; S3 for bond distances and −ICOHP data for $Na_6Cd_{16}Au_7$; Table S4 for bond lengths and −ICOHP values for $Mg_6Cu_{16}Si_7$. Figure S1 shows the measured and calculated powder patterns for $Na_6Au_7Cd_{16}$; Figure S2, the minimum phase field about $Na_6Au_7Cd_{16}$; Figure S3 details the polyhedral environments of all atoms therein; Figure S4 shows the full LMTO DOS and COHP results for $Na_6Cd_{16}Au_7$ that result with Cd 4d orbitals in basis set. This material is available free of charge via the Internet at http://pubs.acs.org.

AUTHOR INFORMATION

Corresponding Author

*E-mail: jcorbett@iastate.edu.

ACKNOWLEDGMENT

The authors are indebted to Gordon J. Miller for advice on several theoretical matters. This research was supported by the Office of the Basic Energy Sciences, Materials Sciences Division, U.S. Department of Energy (DOE). Ames Laboratory is operated for DOE by Iowa State University under contract No. DE-AC02-07CH11358.

REFERENCES

(1) Corbett, J. D. *Inorg. Chem.* **2010**, *49*, 13.
(2) Corbett, J. D. In *Chemistry, Structure and Bonding of Zintl phases and Ions*; Kauzlarich, S., Ed.; VCH Publishers: New York, 1996; Chapter 3.
(3) Corbett, J. D. *Angew. Chem., Int. Ed.* **2000**, *39*, 670.
(4) Pyykkö, P. *Chem. Rev.* **1988**, *88*, 563.
(5) Liu, S. F.; Corbett, J. D. *Inorg. Chem.* **2004**, *43*, 2471.
(6) Liu, S. F.; Corbett, J. D. *Inorg. Chem.* **2004**, *43*, 4988.
(7) Li, B.; Corbett, J. D. *J. Am. Chem. Soc.* **2006**, *128*, 12392.
(8) Lin, Q.; Corbett, J. D. *Inorg. Chem.* **2007**, *45*, 8722.
(9) Dai, J.-C.; Corbett, J. D. *Inorg. Chem.* **2007**, *46*, 4592.
(10) Zachwieja, U. *Z. Anorg. Allg. Chem.* **1995**, *621*, 1677.
(11) Zachwieja, U. *J. Alloys Compd.* **1996**, *235*, 7.
(12) Li, B.; Corbett, J. D. *Inorg. Chem.* **2005**, *44*, 6515.
(13) Henning, R. W. Ph.D. Dissertation, Iowa State University, Ames, IA, 1998.
(14) Henning, R. W.; Corbett, J. D. *J. Alloys Compd.* **2002**, *338*, 4.
(15) Harms, W.; Dürr, I.; Röhr, C. *Z. Naturforsch.* **2009**, *64b*, 471.
(16) (a) Rayaprol, S.; Pöttgen, R. *Phys. Rev. B* **2006**, *73*, 214403. (b) Schappacher, F. M.; Hermes, W.; Pöttgen, R. *J. Solid. State. Chem.* **2009**, *182*, 265.
(17) Doğan, A.; Hoffmann, R.-D.; Pöttgen, R. *Z. Anorg. Allg. Chem.* **2007**, *633*, 219.
(18) Tappe, F.; Pottgen, R. *Z. Naturforsch.* **2009**, *64b*, 184.
(19) Schappacher, F. M.; Rodewald, U. C.; Pottgen, R. *Z. Naturforsch.* **2008**, *63b*, 1127.
(20) Harms, W.; Dürr, I.; Daub, M.; Röhr, C. *J. Solid State Chem.* **2010**, *183*, 157.
(21) Lin, Q.; Corbett, J. D. *Inorg. Chem.* **2007**, *46*, 8722.
(22) Bergman, G.; Waugh, J. L. T. *Acta Crystallogr.* **1956**, *9*, 214.
(23) Nyman, H.; Andersson, S. *Acta Crystallogr.* **1979**, *A35*, 580.
(24) Häussermann, U.; Wörle, M.; Nesper, R. *J. Am. Chem. Soc.* **1996**, *118*, 11789.
(25) Zhak, O. V.; Kuz'ma, Y. B. *J. Alloys Compd.* **1999**, *291*, 175.
(26) Zhang, Q. A.; Liu, Y. J.; Si, T. Z. *J. Alloys Compd.* **2006**, *417*, 100.
(27) Li, B.; Corbett, J. D. *Inorg. Chem.* **2007**, *46*, 6022.
(28) *WinXPow 2.10*; Stoe & Cie GmbH: Darmstadt, Germany, 2004.
(29) *SMART*; Bruker AXS, Inc.: Madison, WI, 1996.
(30) Blessing, R. H. *Acta Crystallogr.* **1995**, *A51*, 33.
(31) *SHELXTL*; BrukerAXS, Inc.: Madison, WI, 2000.
(32) Krier, G.; Jepsen, O.; Burkhardt, A.; Andersen, O. K. *TB-LMTO-ASA Program*, version 4.7; Max-Planck-Institut für Festkörperforschung: Stuttgart, Germany, 1995.
(33) Jepsen, O.; Andersen, O. K. *Z. Phys. B* **1995**, *97*, 35.
(34) Dronskowski, R.; Blöchl, P. E. *J. Phys. Chem.* **1993**, *97*, 8617.
(35) Häussermann, U.; Svensson, C.; Lidin, S. *J. Am. Chem. Soc.* **1998**, *120*, 3867.
(36) Kaskel, S.; Dong, Z.-C.; Klem, M. T.; Corbett, J. D. *Inorg. Chem.* **2003**, *42*, 1835.
(37) Chabot, B.; Cenzual, K.; Parthe, E. *Acta Crystallogr.* **1980**, *B36*, 7.
(38) Grytsiv, A.; Ding, J. J.; Rogl, P.; Weill, F.; Chevalier, B.; Etourneau, J.; Andre, G.; Bouree, F.; Noel, H.; Hundegger, P.; Wiesinger, G. *Intermetallics* **2003**, *11*, 351.
(39) Gupta, S.; Meyer, G.; Corbett, J. D. *Inorg. Chem.* **2010**, *49*, 9949.
(40) Li, B.; Kim, S.-J.; Miller, G. J.; Corbett, J. D. *Inorg. Chem.* **2009**, *48*, 6573.
(41) Miller, G. J.; Lee, C.-S.; Choe, W. In *Inorganic Chemistry Highlights*; Meyer, G., Naumann, D., Wesemann, L., Ed.; Wiley-VCH Publishers: New York, 1996; Chapter 2.
(42) Pearson, R. G. *Inorg. Chem.* **1988**, *27*, 734.